Pore Diffusion in Silver Catalysts

SHINOBU MASAMUNE and J. M. SMITH

Northwestern University, Evanston, Illinois

Diffusion rates were measured at atmospheric pressure and room temperature for helium and nitrogen in pelleted silver catalysts. Pellets were prepared from three silver salts giving different micropore characteristics. The data showed that the diffusion was of the bulk type and that the micropores had no effect, indicating that mass transfer was predominantly in the macropore region. For each kind of material data were obtained for five pellet densities corresponding to macropore volume fractions from 0 up to 0.7.

Effective diffusivities and labyrinth factors ψ were evaluated and found to increase with macropore porosity. The linear relationship between ψ and void fraction proposed by Buckingham for diffusion through soils fitted the data at high void fractions. A generalized form of the Maxwell equation containing three constants was derived. A single-constant form of this expression agreed reasonably well with the measured results over the entire range of macropore volume fraction.

As the problem of reactor design for catalytic reactions has received more exhaustive study, interest has increased in pore diffusion rates. While there have been several studies of mass transfer in individual, porous catalysts and carriers (*6, 7, 10, 11, 13, 14, 15*), sufficient information has not become available to relate the effective diffusivity to the physical properties of the solid phase. This development is necessary before it will be possible to predict mass transfer rates in a given catalyst and hence evaluate the importance of pore diffusion in the over-all reaction rate.

In part the hindrance to progress in this area is due to lack of knowledge of the structure of porous catalysts. Conversely diffusion data can lead to a better understanding of the nature of the pores in a catalytic material, particularly if measurements are made on porous materials whose properties are changed in a regular way.

The purpose of the present work was twofold: to determine the effect of macropore volume fraction on diffusion rates by studying catalyst pellets of different densities, but prepared from the same microporous powders; to obtain diffusivities for later use in interpretating the significance of diffusion resistance on the over-all rate for a specific reaction. Data were measured for three silver catalysts prepared from salts of phthalic, acedic, and fumaric acids. These catalysts are to be used subsequently for studying the rate of decomposition of formic acid in the gas phase. Since the effect of the properties of the porous solid was of interest, all the measurements were carried out with the helium-nitrogen system. Thus diffusivities were determined for these two gases diffusing countercurrent to each other through the catalyst pellets.

Shinobu Masamune and J. M. Smith are at the University of California, Davis, California.

The diffusion measurements were carried out at atmospheric pressure and room temperature in the apparatus shown in Figure 1 and described in later paragraphs.

PREPARATION AND PROPERTIES OF CATALYST POWDERS

The silver catalysts were prepared in accordance with the method described by Yamanaka (*17*). This consisted of first precipitating silver phthalate (Series I catalyst), acetate (Series II), and fumarate (Series III), and then decomposing the salt in a stream of dry nitrogen.

The powders were obtained by grinding the precipitates and retaining the fraction from 200 to 270 U.S. mesh size (73 to 54 μ).

The silver nitrate crystals were labeled 99.98%. Reagent grade phthalic acetic and fumaric acids were used.

The physical properties of Series I and Series III powders were computed from conventional, nitrogen adsorption isotherms. Series II powder showed a negligible adsorption of nitrogen and hence a very small surface area. The surface areas computed from the B.E.T. equation (*2*) and the Wheeler (*16*) mean pore radii for Series I and III are shown in Table 1.

PREPARATION AND PROPERTIES OF PELLETS

Pellets of five different densities were prepared, with powder of each series, as shown in Table 2. Weighed amounts of powder were compressed into cylindrical stainless steel rings, ½-in. I.D. and ⅜-in. long (Figure 2) with a hand press. The lowest-density pellets of each series, designated as I-1, II-1, and III-1 in Table 2, were not mechanically strong enough to hold together. Filter paper was used on either end of the ring to hold the powder in place. In addition to the mass of the pellet and bulk density Table 2 includes volume fractions of silver, micropores, and macropores. The silver volume fraction was calculated from the mass and total volume (1.21 cc.) of the pellet and the density of silver, 10.5 (*5*). The micropore volume fraction was determined from the pore volume given in Table 1 and the mass and total volume of the pellet. The macropore volume fraction was then obtained by difference in accordance with

$$\epsilon_2 = 1 - \epsilon_s - \epsilon_1 \qquad (1)$$

The densities used were chosen so as to try to obtain a pellet of zero macrovoid fraction (ϵ_2) at the highest density. The pressure required for this maximum density was about 7,900 kg./sq.cm It is observed that the densities chosen gave a range of ϵ_2 values from about 0.7 to 0. For Series II the micropore volume was not known. In this case it was assumed that the pellet of maximum density, II-5, corresponded to a zero value of the macropore volume fraction.

Table 1. Physical Properties of Catalyst Powders

	Series I (from silver phthalate)	Series III (from silver fumarate)
Pore volume, V_g cc./g.	0.194	0.138
Surface, area, S_g, sq. m./g.	25.8	5.5
Mean pore radius, r, Å.	150	500

DIFFUSION APPARATUS

The experimental equipment for measuring the counterdiffusion rates through the porous samples was the same as that employed by Henry et al. (*6*), except that the pellets were contained in the stainless steel rings as shown in Figure 2. Pure nitrogen and pure helium flowed past the ends of the cylindrical sample as illustrated in the schematic diagram of the equipment, Figure 1. The pressure on both faces was maintained the same, approximately atmospheric, by the connecting manometer P(3). The diffusion rates were determined directly by measuring, through flow meters F(1) and F(6), the flow rate of pure helium or nitrogen required to give the same composition as the mixtures emerging from the diffusion cell. In addition to the diffusion rates this information also determined the composition of the gas on each side of the pellet for use in Equation (4) to calculate effective diffusivities. The composition of the mixtures were determined in the two thermal conductivity cells shown at the far right side of Figure 1. This procedure was equivalent to calibrating the thermal conductivity cells for each run and thus eliminated errors due to changes in cali-

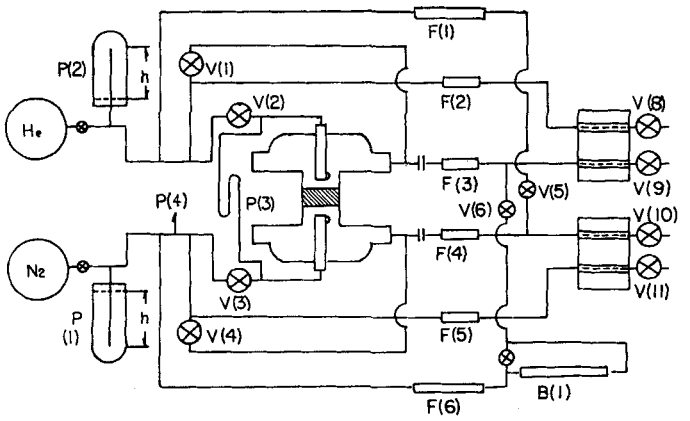

Fig. 1. Schematic diagram of diffusion apparatus.

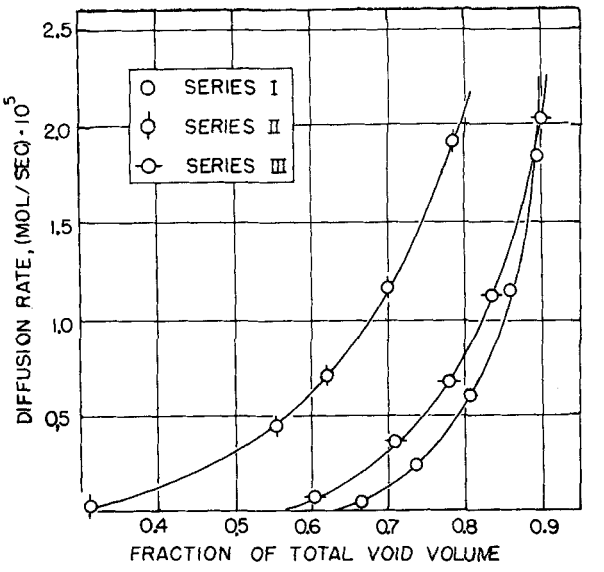

Fig. 3. Diffusion rate of helium vs. total void volume fraction.

bration with time. A complete description of the equipment in Figure 1 and the method of operation is given by Henry (6). The capillary tube flow meters F(1) to F(6) were calibrated with soap film meters. Repeat calibration during the course of the runs indicated a maximum deviation from the average value of less than 1.0%.

Figure 2 shows the steel ring used to hold a sample and the diffusion cell. The helium and nitrogen were introduced tangentially to the end surfaces of the pellet to reduce errors due to diffusion resistance in the gas space on either end of the sample. This was accomplished by closing the end of the entrance tube and attaching perpendicular to it a small diameter, curved, glass tube. The steel ring was mounted in slightly undersized polyethylene tubing and clamped in place to prevent leakage along the outer cylindrical surface. Preliminary tests of the mounting procedure indicated no leakage. The possible resistance of the filter paper on the ends of the sample was checked by making measurements with increasing numbers of pinholes punched in the paper. For all the pellets except the least dense there was no detectable change in diffusion rate as more holes were made in the filter paper. For the least-dense pellet the diffusion rate increased until approximately 25% of the area of the filter paper was void space and was constant for larger void fractions. The data for the least-dense pellet of each series were corrected with this information.

DIFFUSION RESULTS

The observed diffusion rates were in the form of cubic centimeters per minute at the measured room temperature and pressure. These data, converted to moles per second, are shown for helium and nitrogen in Table 2. Two or three runs were made for each pellet and averaged. The maximum deviation of an individual run from the average was less than 2% except for the most dense pellets. For these materials the diffusion rates were much lower and varied considerably from run to run. The decrease in diffusion rate was approximately tenfold from samples I, II, III-4 to I, II, III-5, a decrease much greater than the corresponding reduction in total void fraction ($\epsilon_1 + \epsilon_2$). The mean free path of helium at 25°C. and 1 atm. is about 2,000 Å. and that of nitrogen 800 Å. The I, II, III-5 samples had essentially no macropores, so that diffusion had to be through the micropores. As seen in Table 1 the mean pore diameter of the micropores was less than or of the same magnitude as the mean free path of both helium and nitrogen. Therefore it is indicated that the diffusion in the most-dense pellets was partially of the Knudsen type. This would explain the comparatively low rates shown in Table 2 for pellets I, II, III-5.

The magnitude of the diffusion for the four lower-density pellets is the same as expected for bulk diffusion. This plus the fact that the macropore size is probably in the range 2,000 to 10,000 Å. suggests that in these pellets the diffusion was of the bulk type. The mole ratio of the diffusion rates of helium and nitrogen, except for the highest-density pellet where the results are erratic, is close to theoretical result

$$\frac{N_{He}}{N_{N_2}} = \left(\frac{M_{N_2}}{M_{He}}\right)^{1/2} = 2.64 \qquad (2)$$

for constant pressure, steady state counter diffusion as developed by Hoogschagen (7). Scott (9) has discussed the reasons why countercurrent bulk diffusion rates are not equimolal under constant-pressure steady state conditions and why molal ratios cannot be relied upon to distinguish between Knudsen and bulk diffusion. The analysis of the data on the four lowest-density pellets, presented in the next section, supposes the diffusion to be of the bulk type.

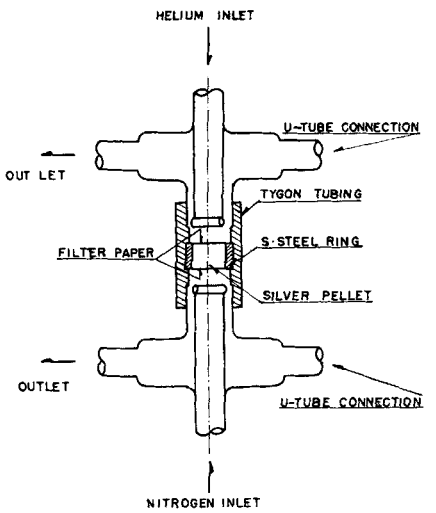

Fig. 2. Detail of diffusion cell.

ANALYSIS OF DATA

The diffusion data for helium are plotted in Figure 3 vs. the total void fraction $\epsilon_1 + \epsilon_2$, and a separate curve is obtained for each series of pellets. The results for nitrogen are similar. However when the data are plotted vs. the macropore volume fraction as in Figure 4 the data for all three series lie on a single curve. Since the micropore void fractions are different for each series, this result suggests that the mass transport occurs almost exclusively by diffusion through the macropores.

The measured diffusion rates may be used to calculate effective diffusivities for the various pellets. Comparison of these values with the bulk diffusivity provides information about the tortuosity of the diffusion path as a function of pellet density.

For a binary gas the net rate of bulk diffusion N_A of component A

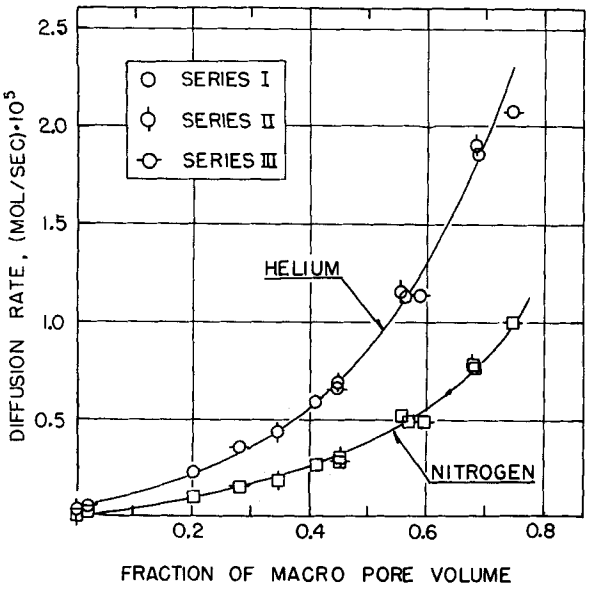

Fig. 4. Diffusion rate vs. macropore volume fraction.

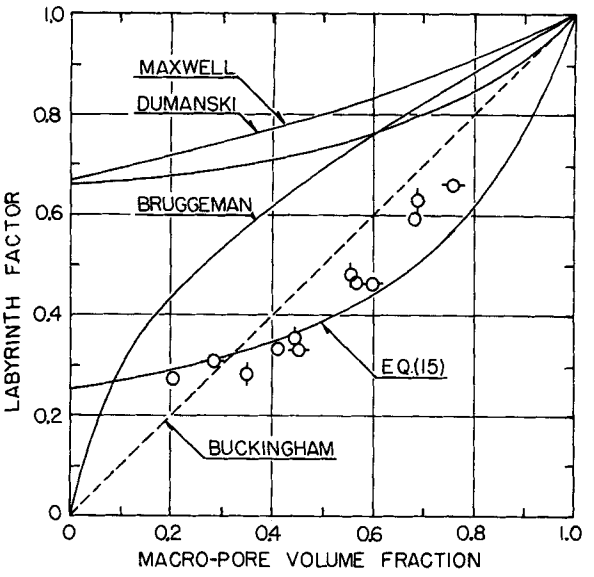

Fig. 5. Effect of macropore volume.

across a stationary plane and per unit area is given (*1*) by the equation

$$N_A = -D_{AB}\frac{p}{RT}\frac{dx_A}{dz} + x_A(N_A - N_B) \tag{3}$$

where D_{AB} is the bulk diffusivity and N_A and N_B are both considered positive quantities. In this expression the ideal gas law has been used to replace the molal concentration in terms of the total pressure. Equation (3) may be applied to the pellet-diffusion data by replacing D_{AB} with an effective diffusivity D_e and integrating across the length $z = L$ of the cylindical pellet. Under the steady state conditions existing in the experiments, N_A, N_B, and the pressure are constant. If the mole fractions are x_{A_0} at $z = 0$ and x_{A_1} at $z = L$, the integrated result is

$$D_e = \frac{RTL}{p}\frac{N_A\left(1-\frac{N_B}{N_A}\right)}{\ln\left[\frac{1-x_{A_1}\left(1-\frac{N_B}{N_A}\right)}{1-x_{A_0}\left(1-\frac{N_B}{N_A}\right)}\right]} \tag{4}$$

Equation (4) has been used to calculate effective diffusivities, and the results are given in Table 2. The fluxes N_{He} and N_{N_2} were obtained by dividing the observed diffusion rates by the total cross-sectional area of the pellet. The mole fraction, pellet length, and pressure and temperature were directly measured.

If the diffusion path through the pellet was in the form of straight pores parallel to the cylindrical walls, the effective diffusivity divided by the void fraction should be equal to the usual bulk diffusivity D_{AB} for the binary system. The deviation from this can be taken as a measure of the tortuosity of the diffusion path through the pellet. Hence it is customary to define a labyrinth factor Ψ (*8*) in accordance with

$$\Psi = \frac{D_e}{\epsilon D_{AB}} \tag{5}$$

Values of Ψ are normally less than unity, indicating a certain degree of tortuosity in the transport through the pellet. Labyrinth factors computed from the average diffusivity are given in Table 2 and in Figure 5. In using Equation (5) the values of D_{AB} corresponding to the observed temperature and pressure were evaluated from the Chapman-Enskog formula (*1*).

Table 2. Catalyst Properties and Diffusion Results

Sample no.	Pellet weight g., W_p	Bulk density g./cc., ρ	Volume fraction Silver ϵ_s	Micropore ϵ_1	Macropore ϵ_2	Diffusion rate Helium, moles/sec., $N_{He} \times 10^{+5}$	Nitrogen, moles/sec., $N_{N_2} \times 10^5$	Effective diffusivity sq. cm./sec., D_e	Labyrinth factor, ψ
Series I									
I-1	1.308	1.08	0.104	0.210	0.686	1.84	0.773	0.222	0.597
I-2	1.791	1.49	0.143	0.291	0.565	1.14	0.496	0.140	0.464
I-3	2.460	2.06	0.195	0.394	0.411	0.589	0.267	0.0736	0.334
I-4	3.350	2.78	0.265	0.535	0.200	0.238	0.108	0.0297	0.277
I-5	4.288	3.55	0.338	0.682	(−0.020)	0.0373	0.0186	0.0487	—
Series II									
II-1	2.770	2.30	0.219	0.097	0.683	1.91	0.789	0.229	0.628
II-2	3.875	3.21	0.306	0.136	0.558	1.16	0.538	0.147	0.491
II-3	4.861	4.03	0.384	0.167	0.449	0.699	0.291	0.0840	0.350
II-4	5.695	4.71	0.450	0.201	0.349	0.437	0.186	0.0532	0.286
II-5	8.772	7.26	0.692	0.308	0	0.0194	0.0108	0.0266	—
Series III									
III-1	1.241	1.03	0.099	0.144	0.757	2.07	1.00	0.266	0.655
III-2	2.076	1.72	0.165	0.239	0.596	1.12	0.494	0.138	0.465
III-3	2.845	2.36	0.225	0.326	0.449	0.658	0.268	0.0788	0.329
III-4	3.697	3.05	0.294	0.426	0.280	0.365	0.165	0.0455	0.303
III-5	5.075	4.21	0.400	0.580	0.020	0.0480	0.0351	0.00772	—

For example at 20°C. and 1 atm. $D_{He\text{-}N_2} = 0.535$ sq. cm./sec. It has been shown earlier that diffusion occurs in the macro rather than the micropores, at least for all except the most dense pellet of each series. Hence the labyrinth factors were evaluated with ϵ_2 in Equation (5).

Figure 5 shows Ψ as a function of macropore volume fraction, and several previously proposed relationships are included as well as the experimental data for the three series of pellets. While some scatter exists in the data, there is no difference between the results for different series. In the absence of any interaction between the gases and the silver this result is expected, since bulk diffusion rates should not depend upon the nature of the solid material.

The earliest and simplest relationship proposed between Ψ and the void fraction is that of Buckingham (3) who suggested in 1904 a linear expression as indicated by the dotted line on Figure 5. His conclusion followed from observations on the diffusion of carbon dioxide and oxygen through soil. Dumanski (4) measured the transport of aqueous sodium sulfate and sodium chloride through gelatin and fitted his results to an equation of the type

$$\Psi = 1 - (1 - \epsilon)^{0.67} \qquad (6)$$

The theoretical relationships of Bruggenman and Maxwell as presented by de Vries (12) and Hoogschagen (7) are also shown in Figure 5:

$$\text{Bruggenman: } \Psi = \epsilon^{1/2} \qquad (7)$$

$$\text{Maxwell: } \Psi = \frac{2}{3 - \epsilon} \qquad (8)$$

Of the previous proposals the linear relationship agrees best with the results of this study. However the trend toward a constant Ψ at low void fractions is not predicted. A modified form of the Maxwell equation which does agree with the data in this region can be derived.

In a general way the effective diffusivity for a porous solid would deviate from the bulk diffusivity because of the decrease in area available for mass transfer and the increase in length of the diffusion path. Suppose that the mean, area void fraction is equal to the volume void fraction times a constant, that is $\bullet C_1$. Suppose also that the effective length of the diffusion path is L_e in comparison with the length L of the pellet. Then, since the diffusion rate is directly proportional to the area and inversely proportional to the path length

$$D_e = D_{AB}\left(\frac{\epsilon C_1}{1}\right)\left(\frac{L}{L_e}\right) \qquad (9)$$

Combining Equations (9) and (5) one gets the following expression for the labyrinth factor:

$$\Psi = \frac{L}{L_e} C_1 \qquad (10)$$

If the pellet is regarded as an assembly of microporous particles of mean size d_p, and if diffusion is assumed to occur only through the macropore spaces between particles

$$L_e = L + n\,(C_2\, d_p) \qquad (11)$$

The mean length porosity, or one-dimensional porosity, is defined

$$\epsilon_L = \frac{L - C_3\, n d_p}{L} \qquad (12)$$

where $C_3\, n d_p / L$ is the fraction of the length that is in the solid phase. The constant C_3 depends upon the shape of the particle; for example $C_3 = 1$ for cubical particles. In general the mean, length porosity will not be the same as the volume void fraction ϵ_2. Again suppose that they are related by a constant C_4, so that Equation (12) may be written

$$\epsilon_2 = \frac{L - C_3\, n d_p}{C_4\, L} \qquad (13)$$

Combining Equations (10), (11), and (13) one gets

$$\Psi = \frac{C_1}{1 + \dfrac{C_2}{C_3}(1 - \epsilon_2\, C_4)} \qquad (14)$$

This equation fits the experimental data shown in Figure 5 very closely, but it contains three arbitrary constants. It reduces to the Maxwell relationship if C_1, C_4, and C_3 are all unity and $C_2 = \frac{1}{2}$. If it is assumed that the length, area, and volume void fractions are equal, Equation (14) contains but one constant, the ratio $C = C_3/C_2$, and may be written

$$\Psi = \frac{C}{C + (1 - \epsilon_2)} \qquad (15)$$

This expression with $C = 1/3$ is plotted in Figure 5 and is seen to agree with the data at low porosities. To fit equally well at high values of ϵ_2 would require a form of Equation (14) in which C_4 is not unity, that is the length void fraction not equal to the volume void fraction. This would mean a two-constant form.

It should be pointed out that the macrovolume fraction gives much better agreement between the Buckingham or modified-Maxwell equations than would be obtained with the total void fraction. In fact the comparatively low values of Ψ presented by Hoogschagen (7) and Wicke and Brotz (15) may be due in part to the use of the total void fraction rather than ϵ_2. Hoogschagen found $\Psi = 0.08$ for an ammonia synthesis catalyst for which $\epsilon_1 + \epsilon_2 = 0.52$, and $\Psi = 0.09$ for a water-gas shift reaction with $\epsilon_1 + \epsilon_2 = 0.60$. Wicke and Brotz determined $\Psi = 0.2$ for a zinc oxide pellet with a total porosity of 0.75.

ACKNOWLEDGMENT

The assistance of Dr. Robert De Baun and Mr. Ben Loper of the American Cyanamid Company in arranging for nitrogen adsorption data on the catalysts is gratefully acknowledged. The financial assistance for this project was provided by the United States Army Research Office (Duke Station), Durham, North Carolina.

NOTATION

A, B	=	components A and B
C_1	=	constants in Equations (9) to (15), dimensionless
C_2	=	constant whose magnitude depends upon the distance the gas molecule has to move perpendicular to the net direction of flow in order to get around the solid particle
D_{AB}	=	bulk diffusivity in the binary system AB sq. cm./sec.
D_e	=	effective diffusivity, sq. cm./sec.
d_p	=	mean size of microporous particle in the pellet, cm.
M	=	molecular weight
N	=	net diffusion flux with respect to a stationary plane, mole/(sec.) (sq. cm.); N is positive regardless of direction of transfer
n	=	number of particles diffusing gas meets in passing through the pellet
p	=	total pressure, atm.
R	=	gas constant, (cc.)(atm.)/(g. mole)(°K.)
$\bar{r}$	=	mean pore radius calculated from equation r $= 2V_g/S_g$, Å
S_g	=	B.E.T. surface area of micropores, sq.m./(g. of pellet)
T	=	absolute temperature, °K.
V_g	=	micropore volume, cc./(g. of pellet)
W_p	=	mass of pellet, g.
x	=	mole fraction
z	=	distance along net diffusion path (axis of pellet), cm.
ϵ	=	volume fraction; ϵ_1 = volume fraction of micropores; ϵ_2 applies to macropores; ϵ_3 to the solid silver phase; ϵ_L is the mean, length void fraction in the macropores.
Ψ	=	labyrinth factor defined by Equation (5), dimensionless
ρ	=	bulk density of catalyst pellet, g./cc.

Subscripts

A,B,N_2,He = gas components, A, B, N_2, and He

0,1 = conditions at entrance and exit of diffusion paths through the pellet

LITERATURE CITED

1. Bird, R. B., W. E Stewart, and E. N. Lightfoot, "Transport Phenomena," pp. 502, 520, Wiley, New York (1960).
2. Brunauer, S., P. H. Emmett, and E. Teller, *J. Am. Chem. Soc.*, **60**, 309 (1938).
3. Buckingham, E., *Bulletin No. 25*, U.S. Dept. of Agriculture, Bureau of Soils (1904).
4. Dumanski, von A., *Kolloid-Z.*, **3**, 210 (1908).
5. "Handbook of Chemistry and Physics," 4 ed., Chemical Rubber Publishing Company, Sandusky, Ohio (1960).
6. Henry, J. P., Jr., Balapa Chennakesavan, and J. M. Smith, *A.I.Ch.E. Journal*, **7**, 10 (1961).
7. Hoogschagen, J., *Ind. Eng. Chem.*, **47**, 906 (1955).
8. Mannegold, E., *Kolloid-Z.*, **82**, 269 (1938).
9. Scott, D. S., *Can J. Chem. Eng.*, to be published.
10. ———, and K. E. Cox, *J. Chimie Physique*, 1010 (1960).
11. ———, *Can. J. Chem. Eng.*, 38, 201 (1960).
12. de Vries, D. A., *Trans. Fourth Internatl. Congress Soil Sci. (Amsterdam)*, **2**, 41 (1950); **4**, 43 (1950).
13. Weisz, P. B., *Z. physik. Chem.*, **11**, 1 (1957).
14. Wicke, E., and R. Kallenbach, *Kolloid-Z.*, **97**, 135 (1941).
15. Wicke, E., and W. Brotz, *Chem. Ing. Technik.*, **21**, 219 (1949).
16. Wheeler, A., "Advances in Catalysis," Vol. 3, p. 250, Academic Press, New York (1951).
17. Yamanaka, T., *Japanese Patents No. 22839 and 22840* (1956).

Manuscript received May 23, 1961; revision received September 15, 1961; paper accepted September 19, 1961.

Thermal Conductivity of Gas Mixtures

HENRY CHEUNG, LEROY A. BROMLEY, and C. R. WILKE

University of California, Berkeley, California

Thermal conductivities of ten gases and selected binary and ternary mixtures of them were measured in a concentric silver cylinder cell over the temperature range from 100° to 540°C. The gases were helium, argon, nitrogen, oxygen, carbon dioxide, methyl ether, and methyl formate.

Correlations based upon empirical equations derived from kinetic theory have been developed for the thermal conductivity of gas mixtures. For mixtures of polyatomic molecules the energy transport is considered in two parts, that is one portion transferred by collision and the other by diffusion. When compared with the experimental data for 226 binary mixtures over temperatures from 0° to 774°C., the conductivity equation proposed in this work shows an average deviation of 2.1%.

Rigorous methods for calculation of thermal conductivity of mixed gases have been developed by Hirschfelder and associates (*11, 13, 14*) based on the classical Chapman-Cowling approach (5). These methods are rather lengthy and laborious to use. A number of more simple semiempirical methods have been proposed which appear to be reasonably accurate (*2a, 21, 23, 24, 25*).

A new method is proposed in this paper based on an extension of the elementary kinetic theory to mixtures. It is believed that shortcomings in the theory are absorbed to a considerable extent by relating the mixture properties to pure component values. On the basis of new experimental data at elevated temperatures which are also reported here it seems that the method may be particularly useful in predicting the temperature dependence of thermal conductivity for mixtures.

DEVELOPMENT OF THE THERMAL-CONDUCTIVITY CORRELATION

In accordance with the kinetic theory the thermal diffusivity, diffusion coefficient, and kinematic viscosity for an ideal gas are of the order of the product of the mean free path and the root-mean-square velocity of the molecules:

$$\frac{\lambda}{\rho C_v} \approx D \approx \frac{\eta}{\rho} \approx \Lambda v \qquad (1)$$

For a single component system

$$\lambda_1 \approx D_{11} \rho_1 C_{v_1} \qquad (2)$$

Thus thermal conductivity is proportional to the rate of movement of the individual molecules within the gas and to the heat capacity per unit volume of the molecules. Analogously for the same gas in a mixture

$$\lambda_{1m} \approx D_{1m} \rho_{1m} C_{v_1} \qquad (3)$$

Dividing Equation (3) by (2) and assuming the proportionality constant to be the same in both expressions one finds

$$\frac{\lambda_{1m}}{\lambda_1} = \frac{D_{1m} \rho_{1m}}{D_{11}\rho_1} = x_1 \frac{D_{1m}}{D_{11}} \qquad (4)$$

The diffusion coefficient D_{1m} is a measure of the rate of movement of any molecule of Type I within a mixture consisting of Type I and molecules of other types. Following Wilke's treatment of the diffusion of a gas into a multicomponent mixture one may write D_{1m} as (35)

$$\frac{1}{D_{1m}} = \frac{x_1}{D_{11}} + \frac{x_2}{D_{12}} + \ldots \qquad (5)$$

Here x_1 and D_{1m} are included, since self-diffusion of molecules of species 1 having different thermal energies is important in the conduction process. After Equation (5) is multiplied through by D_{11} and inverted, the ratio D_{1m}/D_{11} required in Equation (4) is obtained:

$$\frac{D_{1m}}{D_{11}} = \frac{1}{x_1 + \frac{D_{11}}{D_{12}} x_2 + \frac{D_{11}}{D_{13}} x_3 + \ldots} \qquad (6)$$

The thermal conductivity of a mixture is the sum of the conductivities of the individual components; that is

$$\lambda_c = \lambda_{1m} + \qquad (7)$$

As will be explained below, λ_c is that part of the conductivity of a mixture due to conduction only as distinguished from that part due to thermal